  

# A REVIEW ON TURBULENCE MODELS AND NUMERICAL PARAMETERS APPLIED TO IMPINGING JETS

**Daniel Bruno de Vasconcelos Ferreira da Silva**
**Luis Carlos de Castro Santos**
**Luiz Tobaldini Neto**
**Ramon Papa**
Empresa Brasileira de Aeronáutica S.A. - EMBRAER

**Marcelo J.S. De-Lemos***
Departamento de Energia - IEME
Instituto Tecnológico de Aeronáutica - ITA
12228-900 - São José dos Campos - SP – Brazil
* Corresponding author. E-mail: delemos@mec.ita.br

***Abstract.*** *Impinging jets represent an important class of airflow due to their large field of industrial application, however there is a lack of material covering its modeling aspects and concerns. This work presents a comprehensive study on parameters related to the numerical simulation of jets impinging on a flat plate and their influence on the heat transfer coefficient prediction. One CFD finite volume based commercial code was used for the numerical simulation. The application of wall function and low-Reynolds number models for the region close to the wall, as well the nodes density and their distribution in that region were revised. The performance of some turbulence models and their intrinsic parameters adjusting were also studied. Results of temperature fields and Nusselt number are presented and compared to experimental ones. The main goal of this work is to review the range of applicability of certain turbulence models and near-wall region treatment, comparing the behavior of fine and coarse grids.*

***Keywords***. *Impinging jet, turbulence model, Nusselt number, grid sensitivity.*

## 1. Introduction

Impinging jets have a large field of industrial applications because they are an effective way of augmenting the surface heat transfer coefficient. As some examples of their usage, electronic devices cooling, drying processes or wing leading edge anti-ice system can be named. Although many works describing the influence of geometric parameters, like nozzle diameter, distance from nozzle to impinging surface and also the Reynolds number influence can be found in the literature, it is not easy to find related material describing details of the numerical simulation methodology.

The studied case consists on a normally impinging jet on a flat wall. The wall is kept at constant temperature (315K) and the impinging jet is at far field temperature (293K). The objective is to analyze the wall heat transfer to impinging fluid, by calculating the Nusselt number at the wall.

The most interesting aspect of studying geometrically simple and small problems is that experimental results are in most of the cases available, allowing the calibration and validation of the model. Analyzing features of small problems helps understanding more complex cases, as this can be extended to other industrial problems.

In this case, experimental data were taken from the works from Baughn and Shimizu (1989). Additional experimental data were taken from the works from Cooper et al. (1992).

Another relevant aspect in this work is that a massive amount of works about the validation of turbulence models applied to flow features prediction can be found in the literature, while their influence in heat transfer analysis is a field not so well explored.

## 2. Numerical model

### 2.1. Meshes

Four meshes were initially created. All of them are quadrilateral with 130 x 130 elements. The meshes were constructed in a way that its $y^+$ parameter varies in the impinged wall. Maximum values and average values of $y^+$ through the wall are considered, as one can see in the Tab.(1). In this work meshes are frequently referred to after their respective refinement at the wall. So the finest mesh is mesh 1, then mesh 2 and so on until the coarsest one, which is Mesh 4.

Table 1. $y^+$ values for the different meshes

| | Mesh 1 | Mesh 2 | Mesh 3 | Mesh 4 |
|---|---|---|---|---|
| $y^+$ (average) | 0.2 | 0.6 | 1.7 | 5.6 |
| $y^+$ (maximum) | 0.8 | 2.7 | 7.9 | 29.6 |

It should be remembered that $y^+$ is not a fixed geometrical quantity. Once it is function of the position of the center of the first cell and of the flow velocity at this point, it is a solution dependent parameter. Although the size of the first element, at the wall neighborhood, was thought to be scaled with a fixed rate from mesh to mesh, from Table 1 one can see it did not reflect this way on the $y^+$ values.

From Fig.(2) it is possible to see that the impinged wall region, as well as the duct region, is more refined and that the far field region is coarser.

The proposal of this work was to analyze the turbulence models sensitiveness to the $y^+$ variation. Thus, an important issue in the mesh generation procedure is that it must be carefully done in a way that no other parameter but $y^+$ varies. However, small variations in the point distribution are unavoidable in order to keep the elements rate of growth without distortions.

Wall treatment requires special attention when dealing with turbulent flows. In convective heat transfer, the adequate wall treatment is a key question in predicting correct values.

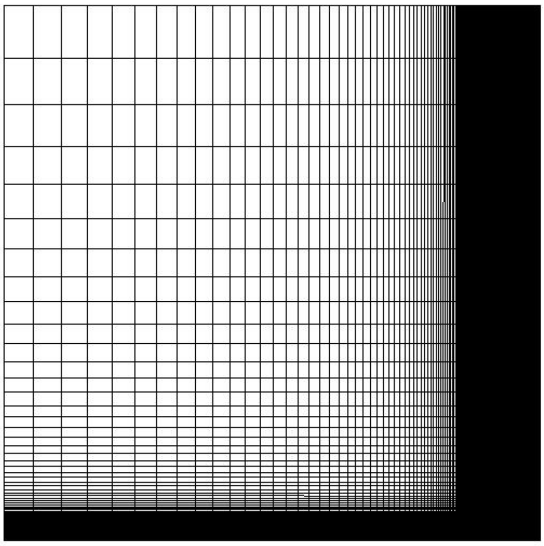

Figure 1. Mesh 4 – Node distribution.

**2.2. Boundary conditions**

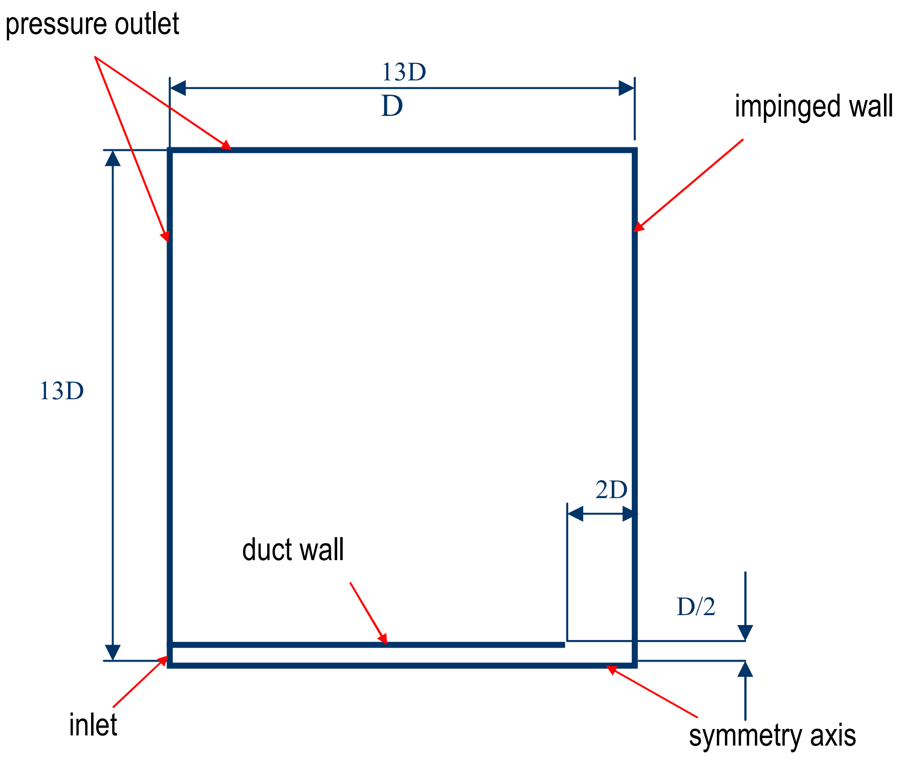


Figure 2. Problem geometry.

The duct is positioned at a distance of two diameters from the impinged wall. Note that the duct has thus 11 diameters, what is enough to guarantee the complete flow development before the duct outlet. The flow conditions at the duct inlet is by itself an interesting study once the Nusselt number distribution at the impinged wall is greatly influenced by the turbulence conditions at the duct inlet as it will be shown later. The lack of information concerning the flow conditions at the inlet used in the experimental procedures brought up a problem by setting up the boundary conditions, in special that required for the turbulence modeling. Having said this, some assumptions had to be made: the turbulence parameters at the duct inlet were chosen to be the hydraulic diameter (0.0403m) and the turbulence intensity (5%). With the diameter of 0.0403m, Mach number is about 0.03, which means that incompressible flow takes place. The inlet boundary condition is defined as a mass-flow inlet, where temperature and gauge pressure are set. Operating pressure is chosen to be the atmospheric pressure (101325 Pa).

The geometry was firstly conceived after the work presented by Vieser, Esch and Menter (2002) in which they propose a simulation domain that is 13 duct diameters large in the axial direction and also 13 diameters large in the radial direction. These values should be enough to guarantee a satisfactory flow development through the pipe (axial direction), as well as to avoid that the possible occurrence of reversed flow in the farfield influences the main flow in the interior of the domain. Fully developed turbulent flow could be assumed for lengths greater than 10 diameters (Incropera and deWitt, 2001).

In the radial direction the region of interest is about 5 diameters large, the same range that can be usually found in the available literature about this problem. The Reynolds number was chosen to be 23000, once experimental results could be easily found for this value.

Figure (1) shows the boundary conditions set up. To achieve a Reynolds number of 23000, based on the tube diameter, the inlet mass flow should be 0.01303 kg/s for the temperature of 293 K.

The duct wall is modeled as a thin, adiabatic wall.

### 2.3. Turbulence modeling

Different turbulence models have a strong influence on impinging jets results, as will be seen further in this text. Understanding how do they influence the calculation of the heat transfer coefficient and consequently of the Nusselt number is not an easy task, but some helpful information can be extracted from the presented results.

### 2.4. Near-wall treatment

Near-wall treatment is one of the key features when modeling convective heat transfer because the wall strongly affects the flow pattern in its surroundings. Fluent uses wall functions for all the k-ε based models. When the mesh is sufficiently fine, k-ω and Spalart-Allmaras turbulence models calculate the flow field throughout the boundary layer.

In Fluent, standard wall functions (SWF) is based on the work proposed by Launder and Spaulding (1972) and it uses the log-law when $y^+$ is greater than 11.25. According to Fluent Inc. (2003), this model should be used very carefully when the flow conditions are considerably different from the ones from where the model was derived.

Non-equilibrium wall functions are an improvement of the above, as developed by Kim and Choudhury (1995). Here, Launder and Spalding's log-law for mean velocity is sensitized to pressure-gradient effects. This wall function employs a two-layer concept in computing the budget of turbulence kinetic energy at the wall-adjacent cells. Comparing it to the former model, non-equilibrium wall functions accounts for some non-equilibrium effects neglected by the standard wall functions.

Enhanced wall treatment is a near-wall model that uses a two-layer model with enhanced wall functions. If the mesh is fine enough – $y^+ \approx 1$ according to Fluent Inc. (2003) – the flow field is computed using the two-layer concept, that solves to the wall. To accomplish the extension of the model to outer regions, the law-of-the-wall is formulated blending linear (laminar) and logarithmic (turbulent) laws-of-the-wall, as proposed by Kader (1993). This approach allows the fully turbulent law to take into account other effects such as pressure gradients or variable properties, accordingly to Fluent Inc. (2003).

## 3. Results

Figures (3), (4), (5) and (6) show the Nusselt number distribution along the wall. The coordinate *r,* representing the radial distance, is adimensionalized by the duct diameter *D*. Red triangles and red circles represent the experimental results, which were used as reference. In this problem the Nusselt number is defined as a function of the duct diameter leading to equation (1), where *h* is the heat transfer coefficient at the impinged wall and *k* is the thermal conductivity of the air.

$$Nu = \frac{h.D}{k} \qquad \text{(Eq.1)}$$

From the presented above, some interesting observations can be made regarding Figs. (3), (4), (5) and (6). For the finest meshes (meshes 1 and 2) the best results were achieved using the v2f model. All models, in mesh 2, presented qualitatively the same behavior as in mesh 1. Some differences are clear, concerning mostly the Nusselt value at the stagnation region. Standard k-ε with all the three wall treatments (standard wall function, enhanced wall treatment and non-equilibrium wall function) shows the greatest Nusselt number over-prediction. Realizable k-ε with non-equilibrium wall function shows also an exaggerated *Nu* over-prediction in both mesh 1 and mesh 2. Spalart-Allmaras, k-ε RNG with enhanced wall treatment and standard *k-ε* with enhanced wall treatment presented also satisfactory results, showing good agreement in the stagnation region. However they were not able to predict the intermediary peak (at r/D=2) that is shown in experimental results. For *r/D* values greater than 2 the experimental results show a decay of *Nu*, but in this region these turbulence models under-predict the Nusselt number. The realizable k-ε with enhanced wall treatment showed the same behavior in all the four meshes, presenting the particular tendency of predicting very low values for Nusselt at the stagnation.

In mesh 3, where *y+* values are relatively greater than in the previous meshes, it is possible to see that the k-ε RNG with standard wall function results are much better than in the previous analysis. Otherwise, the k-ε RNG with enhanced wall treatment slightly over-predicts *Nu* values in the stagnation region, but then it represents the Nusselt number decay after the local maximum point (at r/D = 2) qualitatively well, as in the previous meshes. The v2f model presents also for this mesh the best results, being able to accurately predict the local maximum peak, both its position and its value. The local minimum value, however, is not captured with the same accuracy. One other important issue must also be considered, and it is related to the experimental results scatter. In the stagnation region the difference between the two results shown is almost 20%. This must be taken into account when judging the quality of the numerical results. Nevertheless, both experimental results shown can be considered to be in good agreement, only remarking that they are locally different.

Mesh 4 was conceived to be the most desirable mesh to be used with wall functions ($y^+ \approx 30$). Above this value it begins the region where the log-law becomes valid (up to $y^+ \approx 60$).

A clear trend can be identified with the growth of the *y+* factor, as one note that for both the realizable k-ε and the standard k-ε models, the standard wall function usage brings better results than with the previous meshes. However, the over-prediction of Nusselt number values in the stagnation region is still clear.

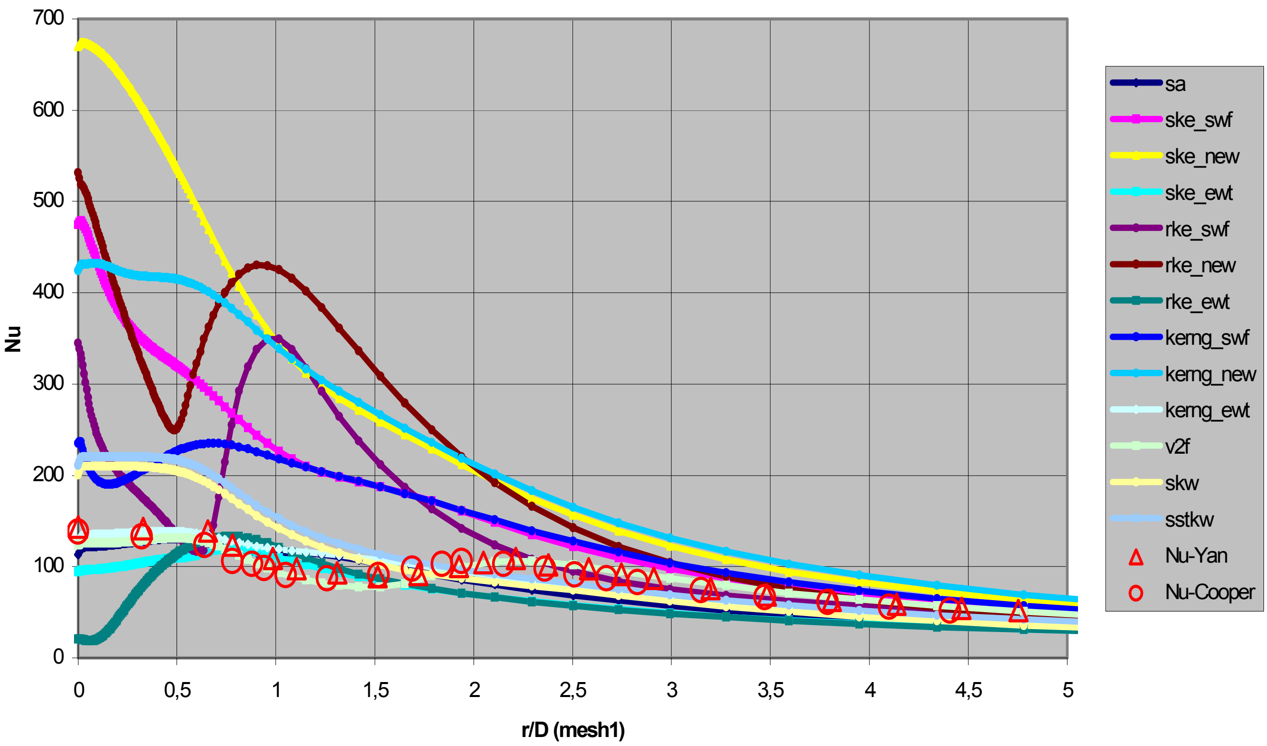


Figure 3. Nusselt distribution along radial distance for mesh 1.

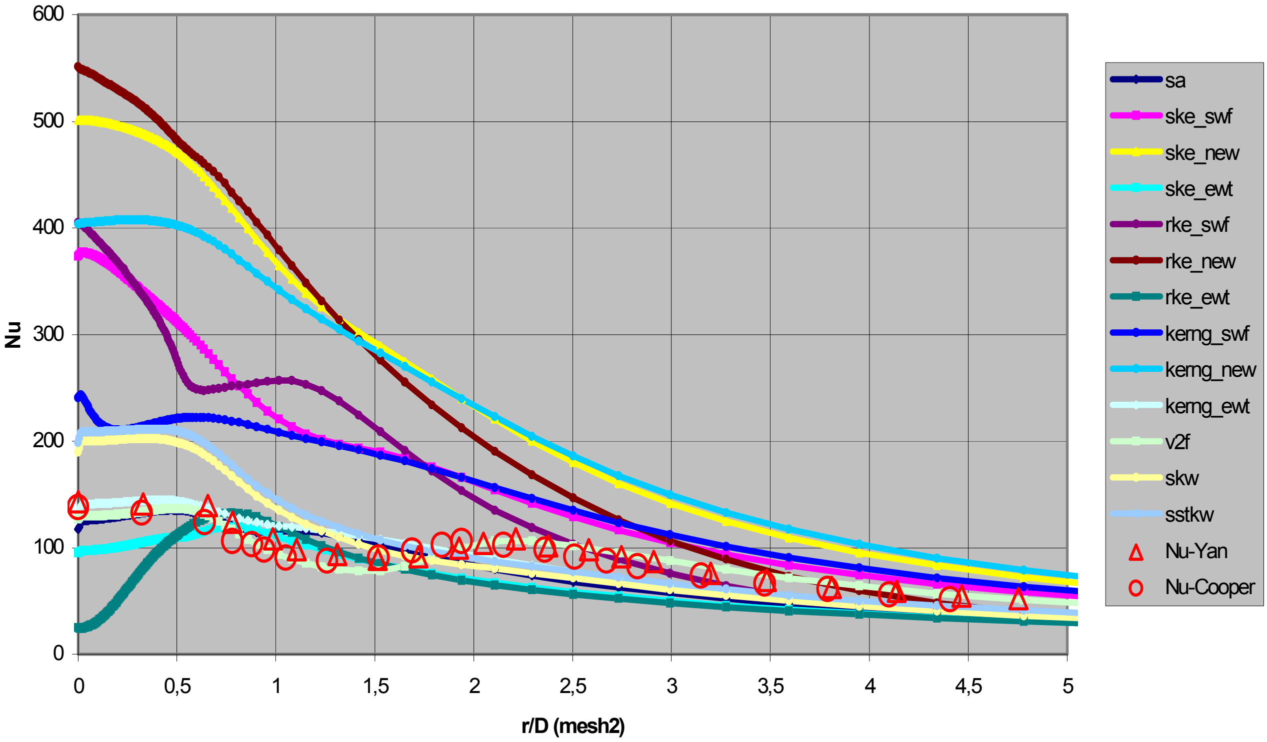


Figure 4. Nusselt distribution along radial distance for mesh 2.

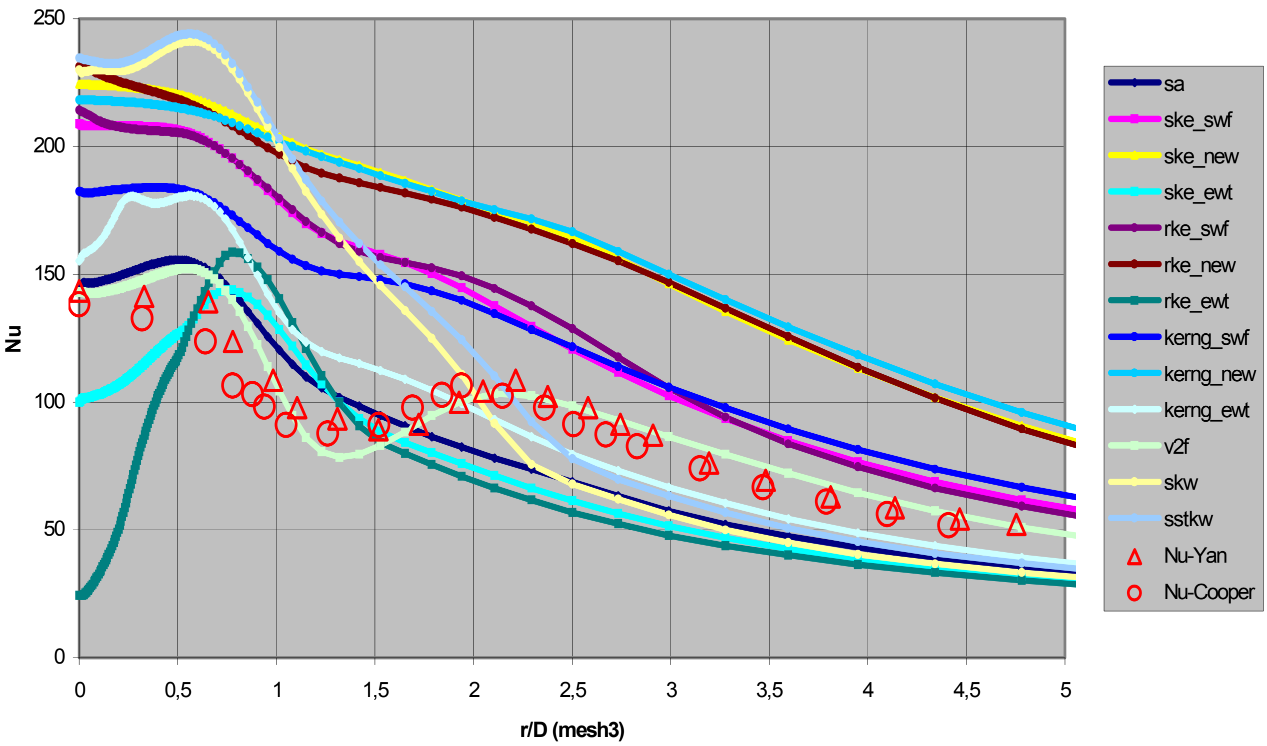


Figure 5. Nusselt distribution along radial distance for mesh 3.

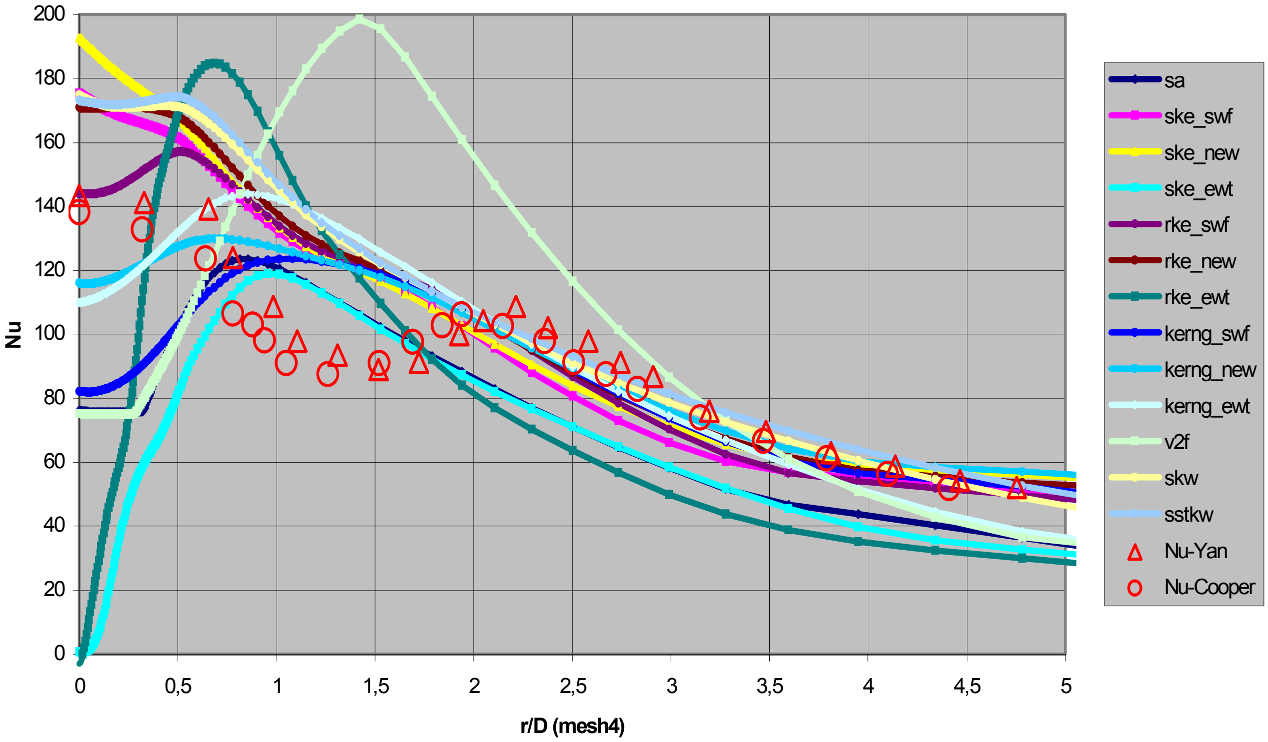


Figure 6. Nusselt distribution along radial distance for mesh 4.

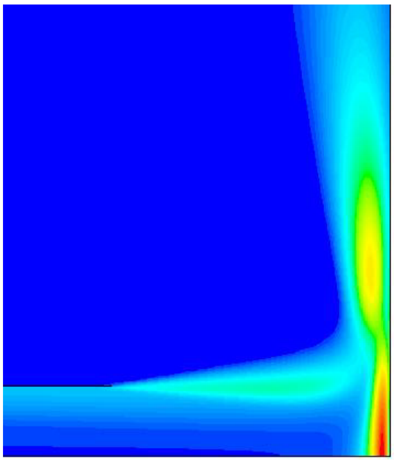

Figure 7. Contours of k (turbulent kinetic energy) – Standard k-e with standard wall function.

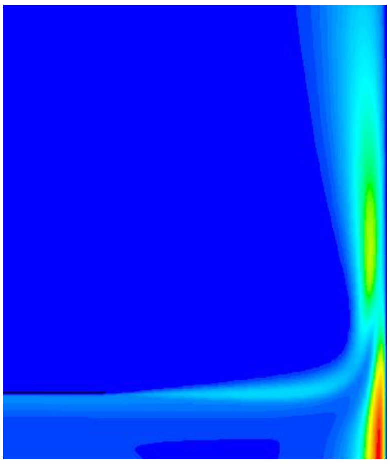

Figure 8. Contours of k (turbulent kinetic energy) – Standard k-w.

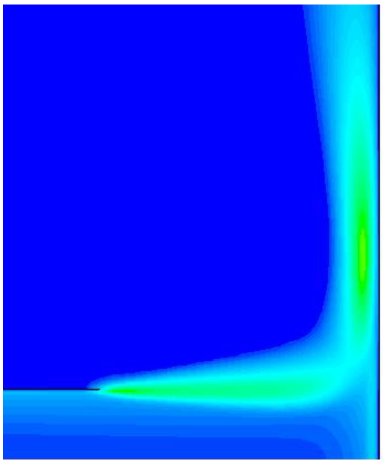

Figure 9. Contours of k (turbulent kinetic energy) – k-ε RNG with enhanced wall treatment.

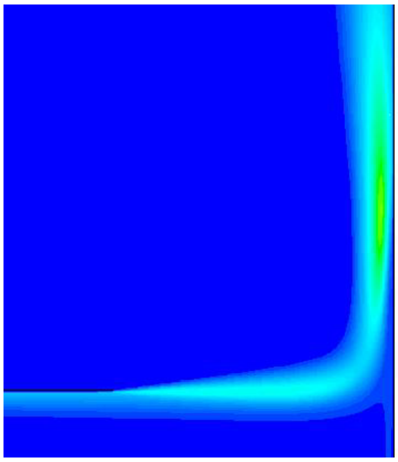

Figure 10. Contours of k (turbulent kinetic energy) – v2f.

In the graphics captions the turbulence models and wall functions abbreviations can be summarized as follow:

ske – standard k-ε
rke – realizable k-ε
kerng – k-ε RNG
swf – standard wall function
new - non-equilibrium wall function
ewt – enhanced wall treatment
skw – standard k-ω
sstkw – SST k-ω
sa – Spalart-Allmaras

One interesting, though not desired, effect can be identified for the v2f and for the Spalart-Allmaras results in mesh 4. Both of them show an extremely accentuated Nusselt number gradient, almost discontinuous, near the stagnation region. As this problem appeared only for this mesh, it is possible to associate it with the maximum discretization at the wall, represented by the $y+$ values that these models support.

In Figs. (7), (8), (9) and (10) contours of $k$, the turbulent kinetic energy, are shown, and are a very useful hint in understanding the lack of effectiveness of the k-ε model in predicting the Nusselt number distribution. The presented contours are taken for the mesh 1 case, where good results were obtained using the v2f and the k-ε RNG with enhanced wall treatment. The colors scale is from blue to red, in crescent order. The k-ε model, and the standard k-ω were chosen as examples of bad results. The v2f and the k-ε RNG with enhanced wall treatment were chosen as examples of good results. From the pictures above is possible to conclude that the over-prediction of k values, what is a typical characteristic of the k-ε model particularly, probably has some influence in the over-prediction of the heat transfer coefficient, here represented by the Nusselt number.

Depending on what kind of application is being considered, it can be of interest to calculate the total heat transfer, as in particular industrial drying processes for example, or knowing the peak heat transfer coefficient, as in hot fluid duct rupture analysis near flammable regions, for example. Calculating the average heat flux over the plate for the experimental results as well as the maximum heat flux ($W/m^2$), they are compared with the numerical results obtained in Tab.(2).

Calculated from the experimental results:

$Q_{average}$=330 $W/m^2$
$Q_{max}$=1600 $W/m^2$

Considering the approximations done in the calculations of the maximum and averaged heat flux for the experimental results, departing from the discrete measured points, and giving an adequate error margin for this kind of heat transfer phenomenon (less than 15%) the numerical results were highlighted in red and blue when inside the fixed error margin.

Table 2. Maximum heat flux values and averaged heat flux values for the different calculations

| | Mesh 1 | | Mesh 2 | | Mesh 3 | | Mesh 4 | |
|---|---|---|---|---|---|---|---|---|
| | $q_{max}$ | $q_{avg}$ | $q_{max}$ | $q_{avg}$ | $q_{max}$ | $q_{avg}$ | $q_{max}$ | $q_{avg}$ |
| **ske_swf** | 4958 | 494 | 6297 | 453 | 2749 | 516 | 2306 | 468 |
| **ske_new** | 6593 | 611 | 8865 | 561 | 2949 | 686 | 2534 | 601 |
| **ske_ewt** | 1576 | 282 | 1567 | 266 | 1890 | 283 | 1564 | 293 |
| **rke_swf** | 5325 | 340 | 4591 | 406 | 2816 | 500 | 2066 | 469 |
| **rke_new** | 7245 | 441 | 6993 | 446 | 3039 | 652 | 2250 | 595 |
| **rke_ewt** | 1745 | 283 | 1753 | 272 | 2085 | 278 | 2430 | 280 |
| **kerng_swf** | 3203 | 522 | 3117 | 480 | 2419 | 545 | 1625 | 487 |
| **kerng_new** | 5360 | 650 | 5686 | 596 | 2869 | 725 | 1708 | 621 |
| **kerng_ewt** | 1904 | 342 | 1822 | 342 | 2376 | 344 | 1891 | 350 |
| **skw** | 2662 | 317 | 2761 | 303 | 3171 | 319 | 2298 | 341 |
| **sstkw** | 2780 | 359 | 2896 | 367 | 3209 | 354 | 2292 | 377 |
| **sa** | 1781 | 306 | 1718 | 307 | 2046 | 306 | 1623 | 305 |
| **v2f** | 1799 | 415 | 1729 | 414 | 2002 | 417 | 2609 | 403 |

Considering the peak value, in the stagnation region, the v2f model and the Spalart-Allmaras could predict it with good accuracy and in the right location for the three cases in which the $y+$ values are close to unity. Other models also produced good values both for the maximum and average values, but the position of the maximum heat transfer may also be an important issue for the designer of the thermal system, in special if it concerns security aspects. Taking that into consideration, the table must be analyzed together with the graphics that shows the *Nu* distribution.

The k-ω models also predicted, within a good tolerance, the average heat flux for all meshes, but failed for the maximum values.

As already noticed from the graphics analysis, the enhanced wall treatment for all the three k-ε models captured the averaged values well, but the peak values, even though in some cases are within the tolerance, they are predicted in the wrong location.

## 4. Conclusions

Even though some simulated results do not match, neither approximate the experimental values, they are useful as a guideline to understand how much is the error one commits by choosing a specific turbulence model instead of other. Taking into account that these calculations have also different computational costs, once the models presented here are 1, 2 or 4-equation models (particularly 3 transport equations and 1 algebraic, for v2f), one must take into account if a more expensive, though more precise, model (as v2f, for example) is really required.

One important aspect is that, for practical reasons, in the industrial environment, CFD users may deal with previously created meshes, which, not necessarily, were created aiming a heat transfer analysis. In this case the user does not have the possibility of controlling the $y+$ values as he desires, or as required for the model to work out reasonably. Another problem is that many times the meshes are already very expensive from the computational point of view and having the *y+* values to fit in such a small range as that required for the v2f model for example, implies an even bigger mesh will be necessary.

As already commented above, the set up of the turbulence modeling in the boundary conditions, in special in the duct inlet for this case, is also a point that must be carefully treated. Once the different models treat the turbulence variables differently, they must be set up in a way that the flows in the inlet for all the models were physically the same. One possible and adequate choice would be determining turbulent intensity and the turbulent viscosity, or viscosity ratio in the inlet. This choice means the same flow, under the same turbulence conditions, is being considered in all the cases, no matter what turbulence model is being used. By plotting the velocity profiles in the duct, in the region near the outlet, at different stations is possible to see that it is practically constant, meaning it can be treated as a fully developed flow. This assures that the turbulent variables have achieved constant values through the duct, what makes it independent from the condition imposed as boundary condition.

As general concluding remarks, the v2f model can be elected as the best alternative if the possibility of having such a fine mesh at the wall exists. This is a 4-equation model, so if convergence time plays a role, and it was not the case for this problem, Spalart-Allmaras (1-equation) is also a good alternative.

Having a fine mesh, the enhanced wall treatment must be applied. It showed good results both for k-ε RNG and the standard k-ε. But for the realizable k-ε instead, the stagnation region was very unsatisfactorily modeled, even using the enhanced wall treatment.

## 5. Acknowledgements

The suggestions and comments of Dr. Guilherme Lara de Oliveira are acknowledged with thanks. MJSDL is thankful to CNPq, Brazil, for supporting his participation in this research effort.

## 6. References

Baughn, J. and Shimizu, S., 1989, "Heat Transfer Measurements From a Surface with Uniform Heat Flux and an Impinging Jet", Journal of Heat Transfer, 111, pp. 1096-1098.

Behnia, M., Parneix, S., Shabany, Y. and Durbin, P.A., 1998, "Numerical Study of Turbulent Heat Transfer in Confined and Unconfined Impinging Jets", International Journal of Heat and Fluid Flow 20.

Cooper, D., Jackson, D.C., Launder, B.E. and Liao, G.X, 1992, "Normally-Impinging Jet from a Circular Nozzle", ERCOFTAC Database Classic Collection.

Fluent Inc., 2003, "Fluent 6.1 Documentation", Vol.2, New Hamsphire, Lebanon, pp. 10.1-10.82.

Incropera, F.P., DeWitt, D., 2001, "Fundamentals of Heat and Mass Transfer", John Wiley & Sons, New York.

Kader, B., 1993, "Temperature and Concentration Profiles in Fully Turbulent Boundary Layers", International Journal of Heat and Mass Transfer, Vol.24, pp.1541-1544.

Kim, S.E. and Choudhury, D., 1995, "A Near-Wall Treatment Using Wall Functions Sensitized to Pressure Gradient", ASME FED, Vol. 217.

Launder, B.E. and Spalding, D.B., 1972, "Lectures in Mathematical Models of Turbulence", Academic Press, London, England.

Spalart, P. and Allmaras, S., 1992, "A One-Equation Turbulence Model for Aerodynamic Flows", Technical Report AIAA-92-0439, American Institute of Aeronautics and Astronautics.

Vieser, W., Esch, T. and Menter, F., 2002, "Heat Transfer Predictions Using Advanced Two-equation Turbulence Models", CFX Technical Memorandum, CFX-VAL10/0602.

Wilcox, D.C., 1998, "Turbulence Modeling for CFD", DCW Industries, Inc., La Canada, California.